Reprinted from *Earthquake Source Mechanics*
Geophysical Monograph 37 (Maurice Ewing 6)

Published in 1986 by the American Geophysical Union.

ON SIMULATING LARGE EARTHQUAKES BY GREEN'S–FUNCTION ADDITION OF SMALLER EARTHQUAKES

William B. Joyner
David M. Boore

U.S. Geological Survey, Menlo Park, California 94025

Abstract. Simulation of ground motion from large earthquakes has been attempted by a number of authors using small earthquakes (subevents) as Green's functions and summing them, generally in a random way. We present a simple model for the random summation of subevents to illustrate how seismic scaling relations can be used to constrain methods of summation. In the model η identical subevents are added together with their start times randomly distributed over the source duration T and their waveforms scaled by a factor κ. The subevents can be considered to be distributed on a fault with later start times at progressively greater distances from the focus, simulating the irregular propagation of a coherent rupture front. For simplicity the distance between source and observer is assumed large compared to the source dimensions of the simulated event. By proper choice of η and κ the spectrum of the simulated event deduced from these assumptions can be made to conform at both low- and high-frequency limits to any arbitrary seismic scaling law. For the ω-squared model with similarity (that is, with constant $M_0 f_0^3$ scaling, where f_0 is the corner frequency), the required values are $\eta = (M_0/M_{0e})^{4/3}$ and $\kappa = (M_0/M_{0e})^{-1/3}$, where M_0 is moment of the simulated event and M_{0e} is the moment of the subevent. The spectra resulting from other choices of η and κ will not conform at both high and low frequency. If η is determined by the ratio of the rupture area of the simulated event to that of the subevent and $\kappa = 1$, the simulated spectrum will conform at high frequency to the ω-squared model with similarity, but not at low frequency. Because the high-frequency part of the spectrum is generally the important part for engineering applications, however, this choice of values for η and κ may be satisfactory in many cases. If η is determined by the ratio of the moment of the simulated event to that of the subevent and $\kappa = 1$, the simulated spectrum will conform at low frequency to the ω-squared model with similarity, but not at high frequency. Interestingly, the high-frequency scaling implied by this latter choice of η and κ corresponds to an ω-squared model with constant $M_0 f_0^4$—a scaling law proposed by Nuttli, although questioned recently by Haar and others.

Simple scaling with κ equal to unity and η equal to the moment ratio would work if the high-frequency spectral decay were $\omega^{-1.5}$ instead of ω^{-2}. Just the required decay is exhibited by the stochastic source model recently proposed by Joyner, if the dislocation-time function is deconvolved out of the spectrum. Simulated motions derived from such source models could be used as subevents rather than recorded motions as is usually done. This strategy is a promising approach to simulation of ground motion from an extended rupture.

Introduction

The lack of near-source recordings of ground motion in large earthquakes has generated interest in methods of simulating such motion for purposes of engineering design. Simulation of ground motion from large earthquakes requires consideration of source, path, and local site effects. Numerous authors have attempted to remove the uncertainty in the path and site effects by using small earthquakes as Green's functions in the simulation of ground motion from larger events [Hartzell, 1978, 1982; Wu, 1978; Kanamori, 1979; Hadley and Helmberger, 1980; Mikumo et al., 1981; Irikura and Muramatu, 1982; Irikura, 1983; Coats et al., 1984; Houston and Kanamori, 1984; Imagawa et al., 1984; Munguiá and Brune, 1984; Hutchings, 1985]. The small earthquakes (henceforth called subevents) ideally are located near the hypothetical source and recorded at the site, but these ideal conditions are commonly relaxed. The method of Green's-function addition not only has the advantage of incorporating wave-propagation effects and local site effects, it also is capable of incorporating the effects of rupture propagation and source-station geometry. In particular the method should model, at least in part, the effect of directivity. Users of the method generally postulate some distribution of subevents over a fault plane and sum them in accordance with an assumed geometry of rupture propagation. Some authors associate with each element of the fault plane a series of subevents spread out in time. Imagawa et al. [1984] filtered subevent records by a filter designed to correct for the difference in rise time between subevent and simulated event.

In this paper we are not advocating the method of Green's-function addition or demonstrating it. Our sole purpose is to show how, in the practical situation, seismic scaling considerations can be used to derive constraints useful in applying the method.

The heterogeneity of earthquake source processes is a crucial issue in the application of the method. Irikura [1983] used the method to simulate ground motion from a shallow magnitude 6.7 earthquake on the assumption of a rupture uniform in both rupture velocity and total dislocation. The resulting motion was deficient at high frequency relative to the observed ground motion, leading to the conclusion that the real rupture was not uniform and forcing a modification of the summing method to enhance the high frequency. Imagawa et al. [1984] attempted to model a different earthquake as a uniform rupture and also came to the conclusion that the rupture was not uniform. Authors other than Irikura have generally included randomness of some sort in their methods for summing subevents. This randomness may be thought to represent a degree of random heterogeneity characteristic of large earthquakes. It also performs an important function in preventing spurious periodicities in the simulated motion resulting from summing over uniform grids in space or over points equally spaced in time. Irikura [1983], who did not use any randomness in his summation, relied on a special smoothing technique to eliminate spurious periodicities.

In the spirit of the original concept of the subevent as a Green's function, the corner frequency of the subevent should be higher than any frequency of interest in the simulated motion. In that case the subevent record will be a true impulse response, and the spectrum of the simulated event will depend on how the subevents are distributed over the fault and in time. The quality of the simulation will depend, accordingly, upon how well the distribution of slip is represented over the fault and in time, in particular, how well the degree and kind of heterogeneity of faulting is represented. In the general case, however, because of limited dynamic range in the subevent records, it may not be possible to use subevents so small that their corner frequencies are higher than any frequency of engineering interest and still maintain the desired bandwidth in the simulated motion. If we wanted to keep the subevent corner frequencies above 3 Hz, we could use subevents no larger than a moment magnitude of about 4; if we wanted to keep the subevent corner frequencies above 10 Hz, we could use subevents no larger than a moment magnitude of about 3. Those who have done simulations by the method of Green's-function addition have generally used much larger subevents, a practice which suggests that it is generally necessary to consider frequencies above the subevent corner.

It is important to note that the effect of directivity will not be correctly modeled at frequencies above the subevent corner frequency unless the angle between the rupture direction and the source-to-station vector is the same for the simulated event as the subevent.

The necessity to consider frequencies above the subevent corner introduces a strong constraint on methods for random summation of subevents, a constraint that, as far as we are aware, has not been explicitly discussed in the literature. At very low frequency the subevent spectra will add coherently and the spectral values of the simulated event will be equal to the sum of the subevent values. At sufficiently high frequency the subevent spectra will add incoherently and the spectral values of the simulated event will be equal to the square root of the sum of squares of the subevent values. These rules in combination with seismic scaling relations form the constraint on methods of random summation. We present here a very simple method of random summation, and use it to illustrate the constraint.

Spectrum of the Simulated Event

In the method η subevents are added together with their start times distributed randomly with uniform probability over the source duration T and their waveforms scaled by a factor κ. Although randomly distributed in time the subevents can be considered to be distributed on a fault with later start times at progressively greater distances from the focus, simulating the irregular propagation of a coherent rupture front. For most of the discussion the waveforms of the subevents are assumed identical. This not only simplifies the discussion, it also corresponds to the practical situation in which generally many times as many subevents are needed as there are small earthquake records available. The case in which the subevents are not identical is considered in the Appendix. For simplicity the distance between source and observer is assumed large compared to the source dimensions of the simulated event. With these assumptions the source spectrum of the simulated event averaged over the ensemble is shown to be

$$S(\omega) = \left\{ \eta \left[1 + (\eta - 1) \, \frac{\sin^2(\omega T/2)}{(\omega T/2)^2} \right] \right\}^{1/2} \kappa S_e(\omega), \quad (1)$$

where $S_e(\omega)$ is the subevent source spectrum. The derivation is given in the Appendix.

At sufficiently high frequencies the shape of the spectrum described by (1) is controlled by the subevent spectrum. Below the corner frequency of the subevent, the subevent spectrum is flat, and the shape of the simulated event spectrum depends upon the quantity in braces in (1). At low frequencies the simulated event spectrum is flat, and at intermediate frequencies it has a trend proportional to ω^{-1}, a consequence of the uniform probability distribution assumed for the random summation, which was a choice made for the sake of simplicity. Other rates of falloff at intermediate frequencies could be obtained by appropriate choice of distribution function. The intersection of the low- and intermediate-frequency trends is at a frequency $f = f_0/\pi$, where $f_0 = 1/T$. We will use the low- and high-frequency limits to constrain methods of summation.

At low frequency (1) simplifies to

$$S(\omega) = \eta \kappa S_e(\omega), \qquad \omega \to 0, \quad (2)$$

and at sufficiently high frequency the second term in square brackets is negligible, and

$$S(\omega) = \sqrt{\eta}\kappa S_e(\omega), \qquad \omega \to \infty. \tag{3}$$

This is just what one should expect; the spectra add coherently at low frequency and incoherently at high frequency. The "sufficiently high" frequency $f(= \omega/2\pi)$ needed for (3) to be applicable is given approximately by

$$fT > \sqrt{\eta}/\pi. \tag{4}$$

Thus we have

$$LF \propto \eta\kappa$$
$$HF \propto \sqrt{\eta}\kappa.$$

where LF and HF are shorthand for the ratios between the spectrum of the simulated event and the subevent at low and high frequency, respectively.

The Constraint

We are now in a position to use the scaling laws of earthquake spectra to determine η and κ. We emphasize the ω-squared model [Aki, 1967; Brune, 1970]. The stochastic version of the ω-squared model proposed by Hanks and McGuire [1981] has been successful in predicting measures of ground motion over a broad range in moment magnitude [Hanks and McGuire, 1981; Boore, 1983; Hanks and Boore, 1984]. For the sake of generality, however, we derive the equations determining η and κ for arbitrary scaling laws. If the displacement spectrum falls off at high frequency as $f^{-\gamma}$, then the high-frequency trend can be written as $M_0(f_0/f)^\gamma$, where M_0 is the seismic moment and f_0 is the corner frequency defined as the frequency at which the low-frequency and high-frequency trends intersect. If the scaling conforms to constant $M_0 f_0^\beta$, then spectral values at high frequency are proportional to $M_0^{1-\gamma/\beta}$, and $HF = (M_0/M_{0e})^{1-\gamma/\beta}$, where M_{0e} is the subevent moment. Noting that $LF = M_0/M_{0e}$ and applying a little algebra gives

$$\begin{aligned} \eta &= \left(\frac{M_0}{M_{0e}}\right)^{2\gamma/\beta} \\ \kappa &= \left(\frac{M_0}{M_{0e}}\right)^{1-2\gamma/\beta}. \end{aligned} \tag{5}$$

For the ω-squared model $\gamma = 2$. If similarity holds, $M_0 f_0^3$ is constant for all earthquakes, and $\beta = 3$. So, for the ω-squared model with similarity

$$\begin{aligned} \eta &= \left(\frac{M_0}{M_{0e}}\right)^{4/3} \\ \kappa &= \left(\frac{M_0}{M_{0e}}\right)^{-1/3}. \end{aligned} \tag{6}$$

Notice that the exponent in the equation for κ is negative. The subevent records must be reduced in amplitude, and correspondingly larger numbers of them added together in order to satisfy the high-frequency and low-frequency requirements simultaneously.

The high-frequency approximation given by (3) is valid above a frequency f_h determined by the inequality (4). Since $f_0 = 1/T$,

$$f_h/f_0 = \sqrt{\eta}/\pi.$$

For the ω-squared model with similarity (6) can be used to obtain

$$\frac{f_h}{f_0} = \frac{1}{\pi}\left(\frac{M_0}{M_{0e}}\right)^{2/3}. \tag{7}$$

With similarity $M_0 f_0^3$ is constant and

$$\frac{f_e}{f_0} = \left(\frac{M_0}{M_{0e}}\right)^{1/3}, \tag{8}$$

where f_e is the subevent corner frequency. Equations (7) and (8) imply that $f_h = f_e$ for a moment magnitude difference of approximately one unit between simulated event and subevent. For larger differences f_h is greater than f_e, and for smaller diferences it is less.

Figure 1 shows the spectrum (light line) of a simulated event, using the values of η and κ given above, for the case in which the difference in moment magnitude between the simulated event and the subevent is one unit. The subevent spectrum is assumed to be

$$S_e(\omega) = \frac{1}{1 + (f/f_e)^2}$$

[Brune, 1970]. The heavy line on Figure 1 shows, for comparision, the spectrum that would result from scaling the subevent spectrum up to the moment of the simulated event in accordance with similarity, that is, with $M_0 f_0^3$ held constant. The value of f_e in Figure 1 is $\sqrt{10} f_0$, and the value of f_h is about $3f_0$, approximately the same, as predicted above. Figure 2 shows the same comparison for the case in which the difference in moment magnitude between the simulated event and the subevent is

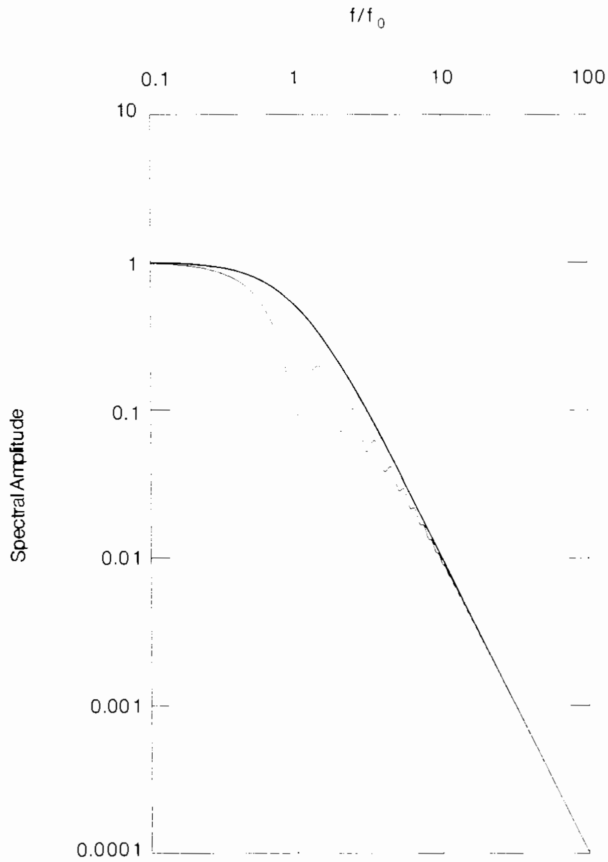

Fig. 1. Spectrum (light line) of the simulated event for a difference of one unit in moment magnitude between simulated event and subevent, compared to the ω-squared spectrum (heavy line) obtained as described in the text. Spectra are normalized to the low-frequency level.

two units. For the case shown in Figure 2, $f_e = 10f_0$, and (4) is satisfied at frequencies above about $30f_0$. The simulated spectra in Figures 1 and 2 are constrained only at the low-frequency and high-frequency limits but are within a factor of two of the target spectra over most of the intermediate-frequency range, indicating that even this oversimplified method of summation gives reasonably satisfactory simulations at intermediate frequencies, at least as long as the magnitude difference between simulated event and subevent does not exceed the two units illustrated in Figure 2. One might hope that more realistic methods of summation would give even better results.

Similarity breaks down for earthquakes larger than that value of moment which corresponds to rupture of the entire width of the seismogenic zone. Joyner [1984] has proposed a scaling law applicable to such events. Consistency with that law can be attained by choosing η and κ such that LF is equal to M_0/M_{0e} and HF is equal to the square root of the ratio of rupture areas.

Applications

The approach used to develop (6) can be applied to show the consequences of other methods of summation. Suppose that η is determined by the ratio of the rupture area of the simulated event to that of the subevent and $\kappa = 1$. In an ω-squared model with similarity, rupture area $A \propto M_0^{2/3}$, so

$$LF = (M_0/M_{0e})^{2/3}$$
$$HF = (M_0/M_{0e})^{1/3}.$$

These relations satisfy the high-frequency but not the low-frequency constraint. The high-frequency part of the spectrum is generally the important part for engineering applications, however, and this method will give satisfactory results in many cases.

Suppose that η is determined by the ratio of the moment of the simulated event to that of the subevent and $\kappa = 1$. Then $\eta = M_0/M_{0e}$, and

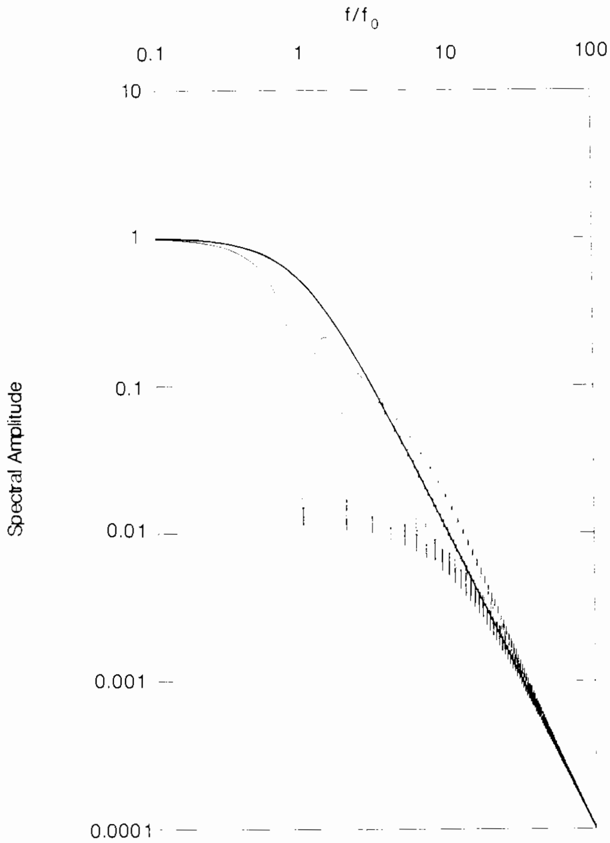

Fig. 2. Spectrum (light line) of the simulated event for a difference of two units in moment magnitude between simulated event and subevent, compared to the ω-squared spectrum (heavy line) obtained as described in the text. Spectra are normalized to the low-frequency level.

$$LF = M_0/M_{0e}$$

$$HF = (M_0/M_{0e})^{1/2}.$$

This satisfies the low-frequency constraint but not the high-frequency constraint demanded by the ω-squared model with similarity. Interestingly, the HF scaling, combined with the high-frequency dependence of $M_0 f_0^2$ for an ω-squared model implies that

$$M_0 f_0^4 = \text{constant},$$

a scaling law proposed by Nuttli [1983], although questioned recently by Haar et al. [1984] and by Atkinson and Boore [1985].

The method of summation proposed by Hadley and Helmberger [1980] is not consistent with the condition expressed by (6). They divide the fault rupture into n elements with n chosen to approximate the ratio of rupture areas between simulated event and subevent. For every element they sum randomly N subevents, each multiplied by ξ/N, where ξ (A_0 in their terminology) is chosen so as to give the correct moment for the simulated event and N is the ratio of the rise time of the simulated event to the rise time of the subevent. If similarity holds, then

$$N = \left(\frac{M_0}{M_{0e}}\right)^{1/3}.$$

If the subevents are equal in moment, then

$$n\xi = \frac{M_0}{M_{0e}}. \tag{9}$$

Since the total number of events $\eta = nN$,

$$\eta = \frac{1}{\xi}\left(\frac{M_0}{M_{0e}}\right)^{4/3},$$

and since the factor κ by which the subevents are multiplied is ξ/N,

$$\kappa = \xi\left(\frac{M_0}{M_{0e}}\right)^{-1/3}.$$

These expressions are equivalent to (6) if and only if $\xi = 1$, but by (9) $\xi = 1$ only if n is equal to the moment ratio between simulated event and subevent. Thus, the method of summation proposed by Hadley and Helmberger [1980] would agree with (6) if n were equal to the moment ratio. They proposed, however, that n be chosen as the ratio of rupture areas.

Simulated Motions as Subevents

The discussion in this paper has been framed in terms of using recorded motions for the subevents, but stochastic simulations could be used just as well. With methods such as those described by Boore [1983] and Joyner [1984], stochastic simulations could be generated representing point sources, and motions from a number of point sources could be added together to represent motion from a fault rupture too large to be treated as a point source. Such an approach may be a particularly efficient way of simulating an extended rupture. One possible source model to be used in the generation of the time series for each subevent is that of Joyner [1984], who proposed a kinematic source model in which the spectrum, with the dislocation-time function deconvolved out, has a high-frequency decay of $f^{-1.5}$. If similarity is assumed, (5) leads to κ equal to unity and η equal to the moment ratio. The dislocation-time function could be included by convolution, as the last step in the simulation process, after the subevent time series had been summed. The concept of using subevents with the dislocation-time function deconvolved out is physically appealing, and the simple addition of subevents using a scale factor of unity has an attractive simplicity.

Appendix

To form the simulated event we take η subevents with spectra $S_{ej}(\omega)$. The subevents all have the same moment, but the spectra are not necessarily identical. We multiply the subevents by κ and add them together with delay times t_j distributed with uniform probability between 0 and T. The expected value of the squared modulus spectrum is

$$S^2(\omega) = E\left\{\left(\sum_{j=1}^{\eta} \kappa S_{ej}(\omega) e^{-i\omega t_j}\right)\cdot\left(\sum_{k=1}^{\eta} \kappa S_{ek}^*(\omega) e^{i\omega t_k}\right)\right\},$$

where E is the expected value operator and * denotes the complex conjugate. S_{ej} and S_{ek} are independent of t_j and t_k, and, for $j \neq k$, t_j is independent of t_k. The probability that t_j takes on a given value is

$$\frac{dt_j}{T} \qquad 0 \le t_j \le T$$

$$0 \qquad \text{otherwise}.$$

$$S^2(\omega) = \sum_{j=1}^{\eta} \int_0^T \frac{dt_j}{T}\, \kappa^2 E\,\{S_{ej}(\omega) S_{ej}^*(\omega)\}$$

$$+ \sum_{j=1}^{\eta} \sum_{\substack{k=1 \\ k\neq j}}^{\eta} \int_0^T e^{-i\omega t_j} \frac{dt_j}{T} \int_0^T e^{i\omega t_k} \frac{dt_k}{T}\, \kappa^2 E\,\{S_{ej}(\omega) S_{ek}^*(\omega)\}.$$

Performing the integrations gives

$$S^2(\omega) = \eta\kappa^2 S_e^2(\omega) + \eta(\eta-1)\frac{\sin^2(\omega T/2)}{(\omega T/2)^2}\kappa^2 E\{S_{ej}(\omega)S_{ek}^*(\omega)\}, \quad \text{(A1)}$$

where $S^2(\omega)$ is the expected value of the squared modulus of the subevent spectrum. If the subevents are identical, then

$$S^2(\omega) = \eta\left[1+(\eta-1)\frac{\sin^2(\omega T/2)}{(\omega T/2)^2}\right]\kappa^2 S_e^2(\omega). \quad \text{(A2)}$$

Taking the square root of (A2) gives (1) of the text. If the subevents are not identical then the spectrum of the simulated event depends upon the statistical properties of the random process represented by the subevent spectra. In the low-frequency limit the subevents must be identical because they have the same moment, and so the low-frequency limit of (A1) is the same as that of (A2). At sufficiently high frequency the second term in (A1) can be neglected, and the high-frequency limit of (A1) is the same as that of (A2)

Acknowledgments. We are grateful to P. Spudich, S. Hartzell, and K. Irikura for careful reviews and valuable suggestions for improving the manuscript. This research was partially supported by a grant from the Nuclear Regulatory Commission.

References

Aki, K., Scaling law of seismic spectrum, *J. Geophys. Res., 72*, 1217–1231, 1967.

Atkinson, G. M., and D. M. Boore, Implications of digital seismograph data for ground motion scaling in eastern North America (abstract), *Earthquake Notes 56*, 4, 1985.

Boore, D. M., Stochastic simulation of high-frequency ground motions based on seismological models of the radiated spectra, *Bull. Seismol. Soc. Am., 73*, 1865–1894, 1983.

Brune, J. N., Tectonic stress and the spectra of seismic shear waves from earthquakes, *J. Geophys. Res., 75*, 4997–5009, 1970.

Coats, D. A., H. Kanamori, and H. Houston, Simulation of strong motion from the 1984 Alaskan earthquake (abstract), *Earthquake Notes, 55*, 18, 1984.

Haar, L. C., J. B. Fletcher, and C. S. Mueller, The 1982 Enola, Arkansas, swarm and scaling of ground motion in the eastern United States, *Bull. Seismol. Soc. Am., 74*, 2463–2482, 1984.

Hadley, D. M., and D. V. Helmberger, Simulation of strong ground motions, *Bull. Seismol. Soc. Am., 70*, 617–630, 1980.

Hanks, T. C., and D. M. Boore, Moment-magnitude relations in theory and practice, *J. Geophys. Res., 89*, 6229–6235, 1984.

Hanks, T. C., and R. K. McGuire, The character of high-frequency strong ground motion, *Bull. Seismol. Soc. Am., 71*, 2071–2095, 1981.

Hartzell, S. H., Earthquake aftershocks as Green's functions, *Geophys. Res. Lett., 5*, 1–4, 1978.

Hartzell, S. H., Simulation of ground accelerations for the May 1980 Mammoth Lakes, California, earthquakes, *Bull. Seismol. Soc. Am., 72*, 2381–2387, 1982.

Houston, H., and H. Kanamori, The effect of asperities on short-period seismic radiation with application to the 1984 Alaskan earthquake (abstract), *Earthquake Notes, 55*, 18, 1984.

Hutchings, L., Modeling earthquakes with empirical Green's functions (abstract), *Earthquake Notes, 56*, 14, 1985.

Imagawa, K., N. Mikami, and T. Mikumo, Analytical and semi-empirical synthesis of near-field seismic waveforms for investigating the rupture mechanism of major earthquakes, *J. Phys. Earth, 32*, 317–338, 1984.

Irikura, K., Semi-empirical estimation of strong ground motions during large earthquakes, *Bull. Disaster Prevention Res. Inst. (Kyoto Univ.), 33*, 63–104, 1983.

Irikura, K., and I. Muramatu, Synthesis of strong ground motions from large earthquakes using observed seismograms of small events, *Proceedings of the 3rd International Microzonation Conference, vol. 1*, 447–458, Seattle, 1982.

Joyner, W. B., A scaling law for the spectra of large earthquakes, *Bull. Seismol. Soc. Am., 74*, 1167–1188, 1984.

Kanamori, H., A semi-empirical approach to prediction of long-period ground motions from great earthquakes, *Bull. Seismol. Soc. Am., 69*, 1645–1670, 1979.

Mikumo, T., K. Irikura, and K. Imagawa, Near-field strong-motion synthesis from foreshock and aftershock records and the rupture process of the main shock fault (abstract), *IASPEI 21st General Assembly*, London, Canada, July 20–30, 1981.

Munguiá, L., and J. N. Brune, Simulations of strong ground motion for earthquakes in the Mexicali-Imperial valley, *Earthquake Engineering Research Institute*, Workshop on Strong Ground Motion Simulation and Earthquake Engineering Applications, Los Altos, California, 1984.

Nuttli, O. W., Average seismic source-parameter relations for mid-plate earthquakes, *Bull. Seismol. Soc. Am., 73*, 519–535, 1983.

Wu, F. T., Prediction of strong ground motion using small earthquakes, *Proceedings of the 2nd International Microzonation Conference, vol. 2*, 701–704, San Francisco, 1978.